ELSEVIER

Journal of Chromatography A, 919 (2001) 231–244

JOURNAL OF CHROMATOGRAPHY A

www.elsevier.com/locate/chroma

Retention and mass transfer characteristics in reversed-phase liquid chromatography using a tetrahydrofuran–water solution as the mobile phase

Kanji Miyabe[a], Sayuri Sotoura[a], Georges Guiochon[b,c,*]

[a]*Faculty of Education, Toyama University, 3190, Gofuku, Toyama 930-8555, Japan*
[b]*Department of Chemistry, The University of Tennessee, 552 Buehler Hall, Knoxville, TN 37996-1600, USA*
[c]*Division of Chemical and Analytical Sciences, Oak Ridge National Laboratory, Oak Ridge, TN 37831, USA*

Received 15 January 2001; received in revised form 2 April 2001; accepted 3 April 2001

Abstract

The characteristics of the retention and the mass transfer kinetics in reversed-phase liquid chromatography (RPLC) were measured on a system consisting of a C_{18}-silica gel and a tetrahydrofuran–water (50:50, v/v) solution. These parameters were derived from the first and the second moments of the elution peaks, respectively. Further information on the thermodynamic properties of this system was derived from the temperature dependence of these moments. Some correlations previously established were confirmed for this system, namely, an enthalpy–entropy compensation for both retention and surface diffusion and a linear free-energy relationship. These results are compared with those observed in other similar systems using methanol–water (70:30, v/v) and acetonitrile–water (70:30, v/v) solutions. The contribution of surface diffusion to intraparticle diffusion in C_{18}-silica gel particles was shown to be important. The analysis of the thermodynamic properties of surface diffusion suggests that, in these three RPLC systems, its activation energy is lower than the isosteric heat of adsorption. The nature and the extent of the influence of the mobile phase composition on the parameters describing the retention and the mass transfer kinetics are different but the chromatographic mechanisms involved in RPLC systems appear similar, irrespective of the nature of the organic modifier in the mobile phase. © 2001 Elsevier Science B.V. All rights reserved.

Keywords: Mass transfer; Kinetic studies; Retention behavior; Mobile phase composition; Benzenes; Toluene; Xylenes; Naphthalene

1. Introduction

High-performance liquid chromatography (HPLC) is the most powerful and reliable separation method in most fields of chemistry [1]. It is reported that 70 to 80% of analytical separations are carried out in the reversed-phase (RP) mode [2]. The selection of the most appropriate stationary and mobile phase in RPLC must be based on the purpose and difficulty of the intended separation. Although methanol–water and acetonitrile–water solutions are most frequently used as the mobile phase in RPLC, aqueous solutions of other organic modifiers, e.g., ethanol and tetrahy-

*Corresponding author. Department of Chemistry, The University of Tennessee, 552 Buehler Hall, Knoxville, TN 37996-1600, USA. Tel.: +1-865-9740-733; fax: +1-865-9742-667.
E-mail address: guiochon@utk.edu (G. Guiochon).

0021-9673/01/$ – see front matter © 2001 Elsevier Science B.V. All rights reserved.
PII: S0021-9673(01)00821-4

drofuran (THF), are also available conveniently to alter the retention behavior in RPLC, when needed. However, insufficient information is available regarding the influence of these other organic modifiers on the mass transfer kinetics in RPLC separations.

The dependence of the retention on the mobile phase composition is most frequently studied using the retention factor (k') as a parameter and the experimental data are discussed on the basis of various models of RPLC retention mechanisms. However, knowledge of other thermodynamic properties and of the mass transfer kinetics is essential for a better understanding of these mechanisms. Yet, there are few detailed studies of the kinetics of mass transfer in RPLC systems, by contrast with the vast number of investigations on their retention behavior.

This paper deals with the retention and the mass transfer characteristics of a specific RPLC system consisting of a THF–water (50:50, v/v) solution as the mobile phase and a C_{18}-silica as the stationary phase. Our results regarding the characteristic features of the mass transfer kinetics and the thermodynamics of this RPLC system are compared with those obtained in similar studies made with aqueous solutions of methanol and acetonitrile.

2. Experimental

2.1. Column and reagents

Table 1 lists some relevant physical properties of the C_{18}-silica gel column used. We chose to pack this column with relatively large C_{18}-silica gel particles (ODS-AQ120-S50 from YMC, Kyoto, Japan) in order to make it easier quantitatively to analyze band broadening phenomena and, more specifically, accurately to estimate mass transfer rate parameters. This packing material is normally used for preparative separations. Some physical properties of the base silica gel are as follows: average particle diameter, 53.6 μm; specific surface area, 340 $m^2\ g^{-1}$; average pore diameter, 12.1 nm; specific pore volume, 1.04 $cm^3\ g^{-1}$. The carbon content of the C_{18} packing material is 14.9% (w/w). The density of bonded C_{18} ligands was calculated as ca. 2.3 μmol m^{-2} on the assumption that the concentration of silanol groups on the surface of the base silica gel is 8 μmol m^{-2}.

The mobile phase consisted of a mixture of THF (HPLC grade, Wako, Osaka, Japan) and water. Water was prepared by distilling ion-exchanged water. The volumetric composition of THF in the mobile phase was adjusted to 50%. In this study, we will compare some characteristics of the chromatographic behavior of RPLC systems using aqueous solutions of different organic modifiers, THF, methanol and acetonitrile, as the mobile phase. The concentration of the organic modifier in the last two systems was 70% (v/v). However, the retention of the sample compounds with a 70% (v/v) THF solution was too small to allow an accurate estimate of the parameters of the retention and the mass transfer kinetics. It is known that the elution strength of a 50% (v/v) aqueous solution of THF is approximately the same as that of similar solutions of 70 to 80% (v/v) methanol or of 60 to 70% (v/v) of acetonitrile [3].

Table 1
Physical properties of the C_{18}-silica gel column and experimental conditions

Average particle diameter, d_p (μm)	53.6
Particle density, ρ_p (g cm^{-3})	0.82
Porosity, ϵ_p	0.29
Tortuosity factor, k^2	4.0
Carbon content (%, w/w)	14.9
Column size (mm)	150×6
Mass of packing materials (g)	2.1
Void fraction, ϵ	0.40
Column temperature (K)	288–308
Mobile phase solvent	Tetrahydrofuran–water (50:50, v/v)
Superficial velocity, u_0 (cm s^{-1})	0.06–0.12
Sample compounds	Alkylbenzenes, chlorobenzene naphthalene

Although this elution strength correlation is not exact, it was shown to be approximately valid in the present case. This justifies the choice of the mobile phase composition.

Sample compounds were all reagent grade and were used without further purification.

Sample solutions were prepared by dissolving the sample compounds into the mobile phase solution. Uracil and sodium nitrate were used as inert tracers.

2.2. Apparatus

A high-performance liquid chromatograph pump (PU-1580, Jasco, Tokyo, Japan) was used. A small volume of the sample solution was introduced into the mobile phase stream by using a valve injector (Model 7125, Rheodyne, Cotati, CA, USA). A thermostated water bath was used to maintain column temperature. The concentration of the sample compounds was monitored with an ultraviolet detector (UV-1575, Jasco).

2.3. Procedure

Table 1 lists the selected experimental conditions. Pulse response experiments (i.e., elution chromatography) were carried out at near-zero surface coverage of the sample compounds while changing the column temperature between 288 and 308 K and the volumetric flow-rate of the mobile phase between 1 and 2 $cm^3\ min^{-1}$. A small concentration pulse or perturbation was introduced into the mobile phase stream. The internal porosity of the C_{18}-silica gel particles and the void fraction of the RP column were derived from the pulse response data obtained for uracil and sodium nitrate, both inert tracers.

The required information regarding the retention equilibrium and the mass transfer kinetics was derived from the first and the second moments of the elution peaks, respectively, on the basis of the results of the moment analysis method [1,4–12]. This approach is often preferred to the apical retention time and the peak width to provide reliable estimates of the equilibrium constant and the column height equivalent to a theoretical plate (HETP), respectively. The elution peak is recorded digitally (after A/D conversion) as a series of data points (y) 0.5 s apart. The first moment (μ_1) is the sum of the products of the elution time and the area of each slice divided by the peak area ($\Sigma ty/\Sigma y$). The second central moment (μ_2') is the sum of the products of the area of each slice and the square of the difference between the slice retention time and the first moment divided by the slice area [$\Sigma(t-\mu_1)^2 y/\Sigma y$]. These calculations were made using a BASIC program operating on the integrator (Shimadzu C-R6A). Details on the moment analysis method were published previously [1,4–12] and only basic information is presented below.

The adsorption equilibrium constant (K) can be derived from the first moment (μ_1) of the elution peak [10–12]. The intraparticle diffusivity (D_e) and the axial dispersion coefficient (D_L) can be derived from the second moment (μ_2') after subtracting the contribution of fluid-to-particle mass transfer to band spreading. The fluid-to-particle mass transfer coefficient (k_f) was estimated by the equation of Wilson–Geankoplis [13]. The molecular diffusivity (D_m) of the sample molecules in the mobile phase solvent was derived from those in neat THF and water by applying the Perkins–Geankoplis equation [14]. Although the Wilke–Chang equation is one of the most popular correlations for the estimation of D_m, it could not be used because the association coefficient involved is not available for THF. The values of D_m for the sample molecules in THF and in water were estimated by the Scheibel equation and the Hayduk–Laudie equation, respectively [14]. The contribution of adsorption–desorption kinetics at actual adsorption sites to μ_2' was assumed to be negligibly small in RPLC [15]. It was also assumed that intraparticle diffusion consisted of two parallel contributions, those due to pore diffusion and to surface diffusion, respectively [8,9]. The surface diffusion coefficient (D_s) was calculated from the result of the subtraction of the contribution of pore diffusion from the intraparticle diffusivity. Pore diffusivity (D_p) was estimated from D_m, the porosity of the C_{18}-silica gel particles (ϵ_p), and the tortuosity factor (k) of the internal pores. The value of k was derived from the second moment of the uracil peak. The experimental retention time and band dispersion were corrected for the contributions of the extra-column volumes between the injection valve and the column and between the column and the detector. These contributions were derived from the results of tracer

experiments made without column. The contributions of μ_1 and μ_2' of the sample pulses introduced at the inlet of the column were ignored because the size of the pulses was extremely small.

Several corrections were made in order to derive surface diffusivities from μ_2'. The influence of these corrections on the precision of the conclusions of this study should be considered. As mentioned earlier, the contribution of the fluid-to-particle mass transfer to μ_2' was subtracted beforehand during the determination of D_e. An uncertainty in the estimation of k_f affects the results of the second moment analysis. In this study, k_f was estimated by the Wilson–Geankoplis equation. For instance, a value $k_f=3.4\cdot10^{-2}$ cm s^{-1} was obtained for benzene at 298 K, when the superficial velocity (u_0) of the mobile phase is 0.12 cm s^{-1}. According to the equation proposed by Kataoka et al. [16], another value, $k_f=2.6\cdot10^{-2}$ cm s^{-1}, was obtained under the same conditions. The corresponding values of D_s were $7.2\cdot10^{-6}$ cm^2 s^{-1} and $5.8\cdot10^{-6}$ cm^2 s^{-1}, respectively. These two values differ by 25%. The results of our study are only slightly influenced by variations in the estimated value of k_f.

The contribution of D_p (pore diffusivity) to D_e (intraparticle diffusivity) was corrected when D_s (surface diffusion coefficient) was calculated from D_e. As mentioned above, D_p was calculated from D_m, ϵ_p, and k. The accuracy of the estimation of D_m affects the accuracy of the estimation of D_s. In this study, D_m for the sample molecules in the THF–water solution was calculated by using the Perkins–Geankoplis, Scheibel, and Hayduk–Laudie equations because the association coefficient in the Wilke–Chang equation is not available for THF [14]. The value of D_m estimated by the set of the above three equations was compared with the value given by the Wilke–Chang equation in order to confirm the accuracy in the estimation of D_m. The set of three equations gives $D_m=9.1\cdot10^{-6}$ cm^2 s^{-1} for benzene in 70% (v/v) methanol in water. The Wilke–Chang equation gives $D_m=8.2\cdot10^{-6}$ cm^2 s^{-1}. These values of D_m are similar. As shown later, the contribution of surface diffusion to the overall mass transfer in the C_{18}-silica gel particles is as much as nearly 95%. Because surface diffusion is the major contribution to intraparticle diffusion, the influence of small variations in D_p (hence in D_m) on the estimate of D_s is small. The error made in the estimates of D_m and D_p influences little the results of this study. Reasonably accurate results were derived for the retention behavior and the mass transfer kinetics in the RPLC system studied.

3. Results and discussion

3.1. First moment analysis

Fig. 1 shows the correlation between the equilibrium constant (K) of the alkylbenzene derivatives in the RPLC system studied and their hydrocarbon surface area (A_s). A_s was calculated by summing up the surface area increments of each group in the sample molecules [17]. The slope of the linear plots in Fig. 1 is related to the decrease in the contact area (ΔA) between the polar molecules of the solvent and the hydrophobic fraction of the surface of contact between the molecules of sample and the C_{18} ligands, as shown by the solvophobic theory. In this theory [18–21], ΔA is assumed to be proportional to A_s of the sample molecules. For the RPLC system

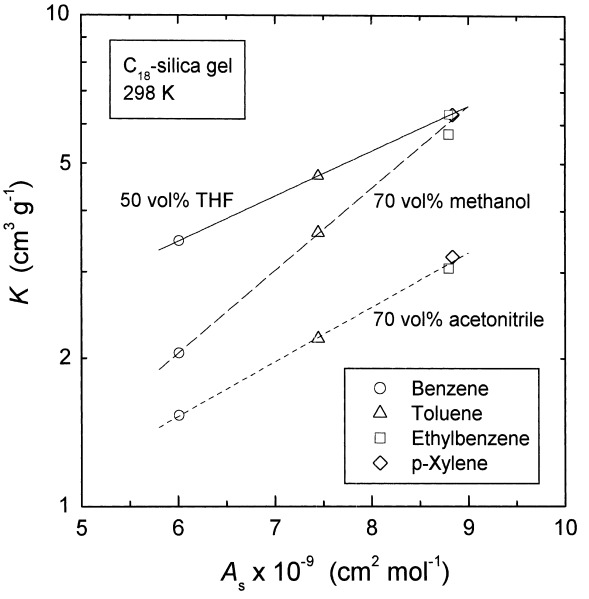

Fig. 1. Correlation of adsorption equilibrium constant with the hydrocarbonaceous surface area of sample molecules.

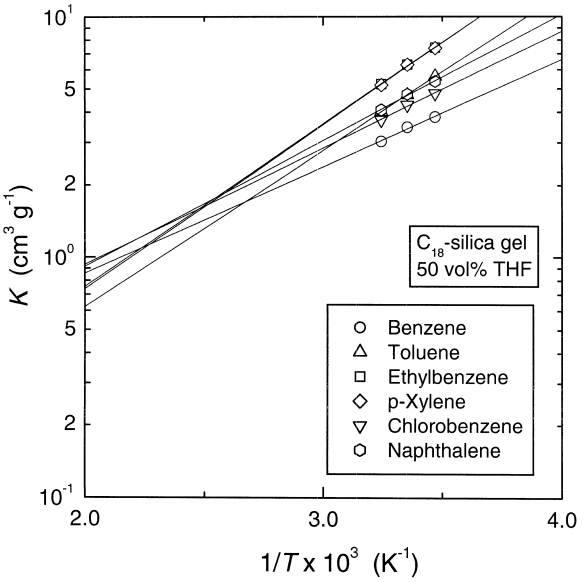

Fig. 2. Van't Hoff's plot of adsorption equilibrium constant.

studied, we found a proportionality constant ($\Delta A/A_s$) equal to 0.2 at 298 K.

Fig. 1 also illustrates, for the sake of comparison, the same linear correlations between ln K and A_s in two other RPLC systems, systems using different mobile phase solvents. As previously reported, values of $\Delta A/A_s$ equal to 0.3 to 0.35 and 0.18 were obtained for methanol (70%, v/v) [11,22] and acetonitrile (70%, v/v) [11,23], respectively. Other values of $\Delta A/A_s$ reported are ca. 0.35 for RPLC on bonded silica with an aqueous buffer as the mobile phase [20] and 0.2 to 0.3 for a system with organic solvents and activated carbon [21]. The value $\Delta A/A_s=0.2$ found in this study suggests that the magnitude of the interactions between the sample molecules and the C_{18} ligands in 50% (v/v) THF is in the low part of the range observed for RPLC systems.

According to the Van't Hoff equation, the isosteric heat of adsorption (Q_{st}) was calculated from the temperature dependence of K (Fig. 2):

$$K = K_0 \exp\left(\frac{-Q_{st}}{RT}\right) \quad (1)$$

where K_0 is K at $1/T=0$ or $|Q_{st}|=0$, R the universal gas constant, and T the absolute temperature. Table 2 lists the values obtained for $-Q_{st}$, values ranging from 8.5 to 13.1 kJ mol^{-1}. These values are of the same order of magnitude as others previously measured and reported [24–30]. They are slightly larger than those obtained for the same compounds in RPLC systems using aqueous solutions of methanol (6.7 to 10.3 kJ mol^{-1}) [31] and acetonitrile (5.8 to 7.1 kJ mol^{-1}) [23].

Table 2 also lists the values of K_0 derived from the intercepts of the linear plots in Fig. 2. The value of ln K_0 is proportional to the entropy change arising from the retention of the sample molecules. The retention processes are accompanied by a decrease of entropy in the system studied. Fig. 3 shows the correlation between K_0 and $-Q_{st}$. Fig. 3 suggests an enthalpy–entropy compensation concerning the retention behavior in the system studied. Such an enthalpy–entropy compensation was reported in other RPLC systems, with a compensation temperature ranging from ca. 500 to 1000 K [32–40]. A compensation temperature of about 400 K was derived from the slope of the solid line in Fig. 3. This value is of the same order of magnitude as previous results [32–34]. The enthalpy–entropy compensation will be discussed in more detail later.

Table 2
Thermodynamic properties of retention equilibrium and surface diffusion in RPLC

Sample	$-Q_{st}$ (kJ mol^{-1})	K_0 (cm^3 g^{-1})	E_s (kJ mol^{-1})	D_{s0} (cm^2 s^{-1})
Benzene	8.5	$1.1\cdot10^{-1}$	15.0	$1.3\cdot10^{-3}$
Toluene	12.5	$3.1\cdot10^{-2}$	18.1	$3.8\cdot10^{-3}$
Ethylbenzene	13.0	$3.3\cdot10^{-2}$	21.0	$9.3\cdot10^{-3}$
p-Xylene	13.1	$3.2\cdot10^{-2}$	18.7	$4.0\cdot10^{-3}$
Chlorobenzene	9.3	$1.0\cdot10^{-1}$	17.3	$2.7\cdot10^{-3}$
Naphthalene	10.0	$8.2\cdot10^{-2}$	21.6	$1.2\cdot10^{-2}$

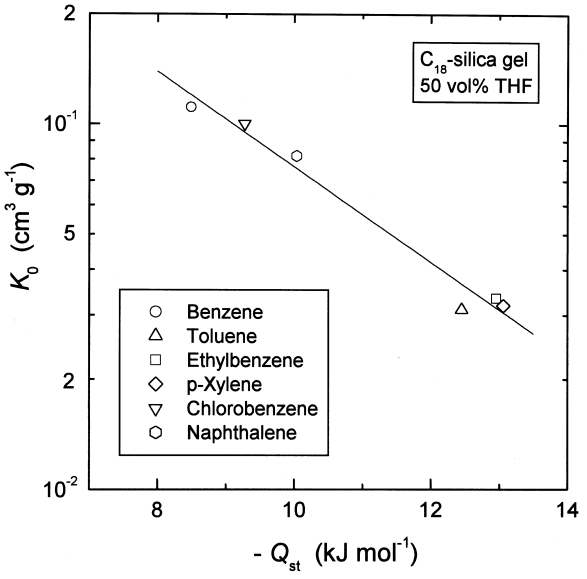

Fig. 3. Enthaply–entropy compensation of retention behavior.

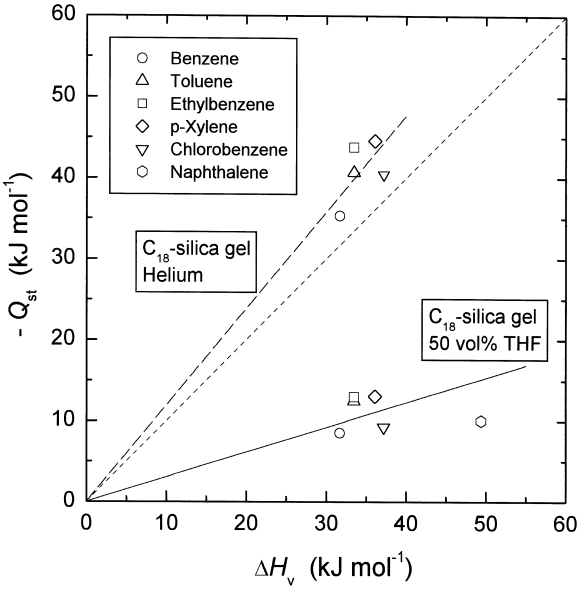

Fig. 4. Plot of isosteric heat of adsorption against heat of vaporization.

The result in Table 2 suggests that the entropy reduction upon adsorption of larger molecules is larger than that of smaller ones. This entropy change is probably correlated with changes in the mobility of both the sample and the solvent molecules, in the solvation of the sample molecules, and in the steric conformation of C_{18} ligands. Further accumulation of reliable experimental data and quantitative analyses of these entropy changes would be necessary for a more detailed study of the retention mechanisms in RPLC, from a thermodynamic point of view.

Fig. 4 shows the correlation between the heat of vaporization (ΔH_v) of the sample compounds and $-Q_{st}$ in either a gas–solid adsorption system or the RPLC system studied. Although a definitive correlation between ΔH_v and $-Q_{st}$ is not a thermodynamic requirement, it appears that $-Q_{st}$ in our RPLC system about 1.2 times as large as ΔH_v in a C_{18}-silica gel/helium system [11,41]. An adsorbate layer in equilibrium with a gas phase is a condensed phase on the surface of the adsorbent. So, its desorption into the gas phase is a physical phenomenon analogous to the vaporization of the same compound from the bulk. However, the desorption of the adsorbate molecules requires more energy than its vaporization because the adsorbed phase is in the potential field generated by the adsorbent surface. The difference between $-Q_{st}$ and ΔH_v is largely due to the interactions between the adsorbate molecules and the surface of the adsorbent. On the other hand, the value of $-Q_{st}$ in the RPLC system is relatively small compared with that found for the gas–solid adsorption system. The smaller value of $-Q_{st}$ in the RPLC system is explained by the influence of the mobile phase solvent on Q_{st} [11]. The ratio of $-Q_{st}$ to ΔH_v in the RPLC system, 0.35, is smaller than that in the gas–solid system, 1.2. The difference between Q_{st} for two similar compounds in the RPLC system is roughly written as follows:

$$\Delta(-Q_{st}) = 0.35\Delta(\Delta H_v) \quad (2)$$

3.2. Second moment analysis

Information on the kinetic processes involved in the C_{18}-silica gel column was provided by the second moment analysis. It is usually assumed that μ_2' consists of the four contributions of as many individual mass transfer processes, namely axial dispersion (δ_{ax}), the fluid-to-particle mass transfer (δ_f), intraparticle diffusion (δ_d), and the actual adsorption process (δ_{ads}) [1,8,9,42]. The influence of δ_{ads} at the actual adsorption sites on band broadening

is negligibly small in RPLC systems because adsorption–desorption is fast compared with the other mass transfer processes [15]:

$$\mu_2' = \frac{2z}{u_0}(\delta_{ax} + \delta_f + \delta_d) \quad (3)$$

The relative importance of the contributions of the other three processes to μ_2' are compared in Fig. 5 for six compounds. The contribution of δ_{ax} is about 30%. The contributions of δ_f and δ_d range between 30 and 40% and 30 and 35%, respectively. Fig. 5 indicates that the contributions of these three kinetic processes to peak spreading are all of the same order of magnitude when the particle size of the RP stationary phase is relatively large ($d_p = 53.6$ μm in this study). This result is very different from what is observed in gas–solid adsorption systems [41], in which case the contribution δ_f was one or two orders of magnitude smaller than δ_{ax} and δ_d. The contribution of δ_d was then more than 75% of the total, suggesting that δ_d had the major influence on μ_2'. By contrast, the values of δ_{ax}, δ_f, and δ_d in Fig. 5 have almost the same order of magnitude. None can be neglected when peak spreading in the C_{18}-silica gel column is analyzed quantitatively from a kinetic point of view.

Intraparticle diffusivity (D_e) is frequently accounted for by assuming parallel contributions of pore diffusion and surface diffusion [8,9], leading to the following relationship:

$$D_e = D_p + \rho_p K D_s \quad (4)$$

where D_p and $\rho_p K D_s$ denote the contributions of pore and surface diffusion to intraparticle diffusion, respectively. As shown in Fig. 6, D_e is one order of magnitude or more larger than D_p, suggesting that the contribution of surface diffusion to the overall mass transfer in the C_{18}-bonded stationary phase is as much as about 95%. Calculations showed the value of D_s to be of the order of 10^{-6} cm^2 s^{-1}. Thus, surface diffusion plays an important role in intraparticle diffusion through C_{18}-silica gel particles and in band broadening on RPLC columns. Intrinsic characteristics of surface diffusion should be clarified in more detail for a better understanding of the mechanisms of this type of diffusive mass transfer.

3.3. Characteristics of surface diffusion in RPLC

It was attempted to correlate D_s with some physico–chemical parameters of the sample molecules in order to derive some useful information on the characteristic features of surface diffusion in RPLC.

Fig. 7 shows the correlation of D_s with a function

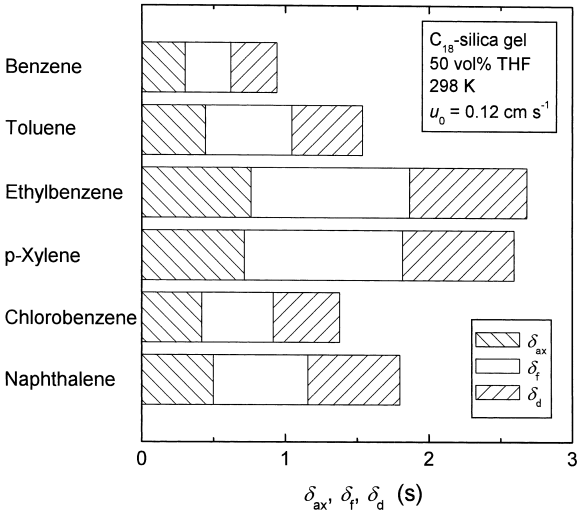

Fig. 5. Comparison of the contributions of axial dispersion, fluid-to-particle mass transfer, and intraparticle diffusion to second moment.

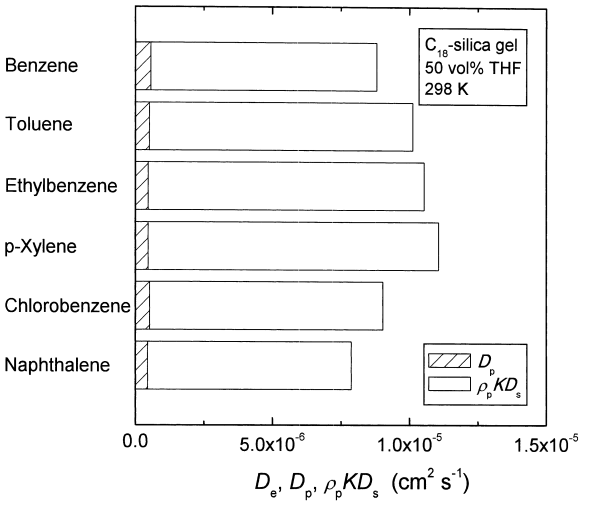

Fig. 6. Comparison of the contributions of pore diffusion and surface diffusion to intraparticle diffusion.

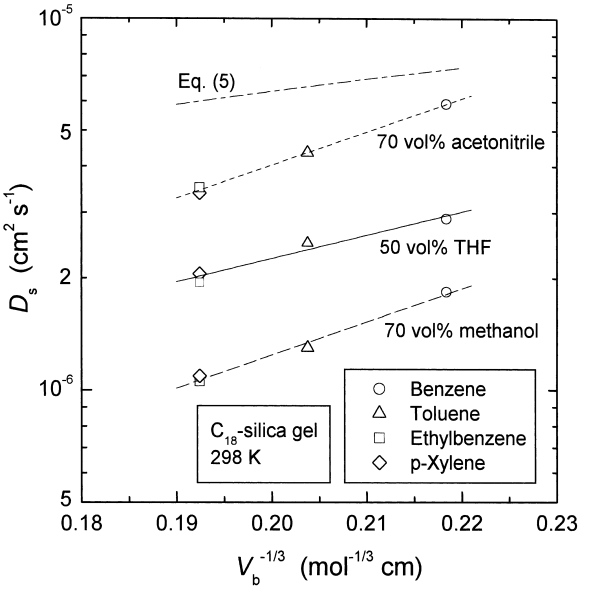

Fig. 7. Plot of surface diffusion coefficient against the molar volume of sample molecules at their normal boiling point. The dot–dashed line represents the correlation calculated by Eq. (5).

of the molecular size of the sample molecules. The following empirical equation was proposed to estimate the diffusivity of a tracer in a binary system involving long-chain hydrocarbons [43]:

$$\frac{10^9 D_{a,sv}\eta_{sv}}{TV_{b,sv}^{2/3}} = \frac{11.96}{V_{b,a}^{1/3}} - 0.8796 \quad (5)$$

where $D_{a,sv}$ is the diffusivity, η the viscosity, and V_b the molar volume of the sample at the normal boiling point. The subscripts a and sv denote the sample molecule and the solvent, respectively. As a first approximation, surface diffusion was assumed to be equal to the tracer diffusion of the sample molecule in *n*-octadecane, the influence of the nature of the mobile phase on surface diffusion being neglected. The dot–dashed line in Fig. 7 illustrates the correlation of $D_{a,sv}$ with $V_{b,a}^{-1/3}$ at 298 K calculated through Eq. (5). Fig. 7 also shows plots of D_s in the RPLC systems previously studied, using 70% (v/v) methanol and 70% (v/v) acetonitrile, versus $V_b^{-1/3}$. The difference between the calculated value of $D_{a,sv}$ and the experimental values of D_s results probably in part from the tortuosity of the surface of the stationary phase, the solvation of both the sample molecules and the C_{18} ligands, and the restricted mobility of the C_{18} ligands due to the chemical bonding of these ligands to the surface of the silica gel.

The results in Fig. 7 also show the importance of the influence of the mobile phase on the surface diffusion of the sample molecules and on their retention behavior. These results falsify the assumption made above, that the nature of the solvent used in the mobile phase has no influence on surface diffusion. As shown in Fig. 7, D_s in the mobile phase solvents increases in the following order: 70% (v/v) methanol < 50% (v/v) THF < 70% (v/v) acetonitrile. This order is different from that of the retention strength, illustrated in Fig. 1, suggesting that the influence of the mobile phase composition on surface diffusion (D_s) and on the retention behavior (K) are different.

A probable explanation for the difference between the values of D_s in the three mobile phases is that surface diffusion should be regarded as the diffusive migration of the sample molecules through a stationary phase consisting of a solution of the C_{18} alkyl ligands in the mobile phase. Tanaka et al. [44] also reported that the dependence of the retention behavior on the mobile phase composition in RPLC could be interpreted by considering that the organic solvent used to make the mobile phase participates into the stationary phase and that the sample molecules seemed to be distributed between the bulk mobile phase and the actual stationary phase solution. Their study of the retention behavior demonstrated the important role of the mobile phase solvent on the separation mechanisms in RPLC. Our study of the mass transfer kinetics of sample molecules along the surface of the C_{18}-silica gel leads to similar conclusions concerning the significant role of the mobile phase solvent.

According to the Arrhenius equation, the activation energy of surface diffusion (E_s) at near-zero surface coverage of adsorbate is given by:

$$D_s = D_{s0} \exp\left(\frac{-E_s}{RT}\right) \quad (6)$$

where D_{s0} is the frequency factor of surface diffusion. Fig. 8 shows such plots of D_s for the different compounds studied, measured with a mobile phase containing 50% (v/v) THF. The values of E_s calculated from the slope of the linear correlations in Fig.

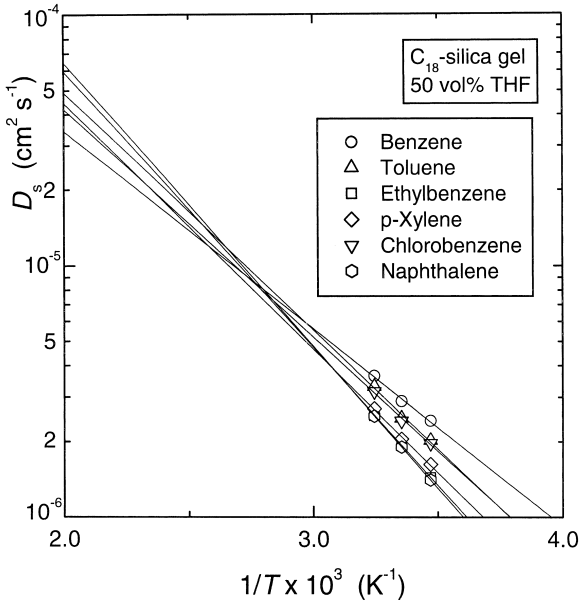

Fig. 8. Arrhenius' plot of surface diffusion coefficient.

8 are between 15.0 and 21.6 kJ mol^{-1}, as listed in Table 2. These values of E_s are larger than those obtained with other organic modifiers, i.e., 19.4 to 23.4 kJ mol^{-1} (70%, v/v, methanol) [31] and 14.6 to 16.6 kJ mol^{-1} (70%, v/v, acetonitrile) [23]. Fig. 9

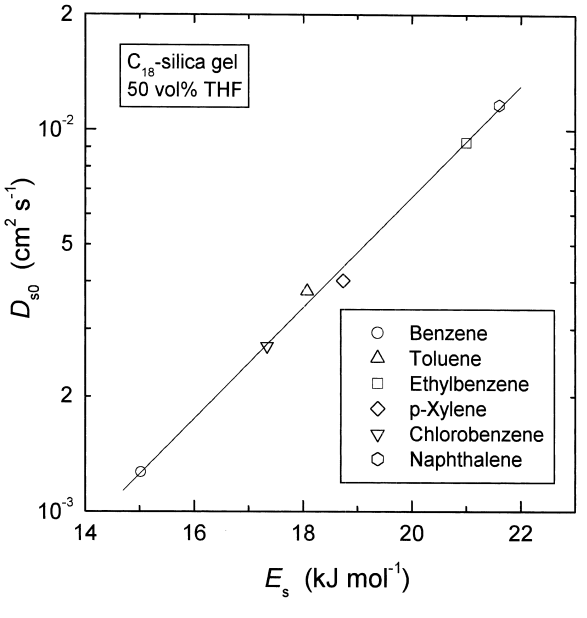

Fig. 9. Enthaply–entropy compensation of surface diffusion.

shows a linear correlation between ln D_{s0} and E_s, suggesting that an enthalpy–entropy compensation is also found for surface diffusion on C_{18}-silica gel [45]. Thus, we found an enthalpy–entropy compensation for both the retention equilibrium and surface diffusion in an RPLC system.

Analysis of the temperature dependence of equilibrium constants or rate coefficients on the basis of the Van't Hoff equation or the Arrhenius equation is the most usual method for estimating the variations of enthalpy (ΔH) and entropy (ΔS) associated with reaction equilibria or kinetic processes. However, Krug et al. [46–48] have shown that it is possible to observe linear correlations between ΔH and ΔS estimated from the Van't Hoff plot even when no enthalpy–entropy compensation takes place. Such linear correlations could arise merely from the compensation of the errors made in the determination of ΔH and ΔS from the Van't Hoff or the Arrhenius correlation. They showed that the correlation coefficient and the slope of the linear regression that would originate from this statistical compensation effect are close to unity and to the harmonic mean of the experimental temperatures (T_{hm}), respectively. Krug et al. [46–48] suggested four different methods to determine whether a linear correlation observed between ΔH and ΔS is caused by an actual physico–chemical phenomenon or arises from the statistical pattern generated by experimental errors. In this study, we examine the experimental data plotted in Figs. 3 and 9 concerning the retention equilibrium and surface diffusion in the RPLC system according to the four methods recommended by Krug et al. [46–48].

(1) If an important physico–chemical effect is really present, the plot of ΔH vs. ΔG_{Thm} (the Gibbs free energy change at T_{hm}, see above) should be linear. The compensation temperature ($T°$) can then be derived from the slope of this linear plot [46–48].

Fig. 10a and b show the plots of ΔH vs. ΔG_{Thm} for the retention equilibrium and the surface diffusion, respectively. These plots were calculated from the slope and the intercept of the linear regression of ln K vs. $\{1/T-\langle 1/T\rangle\}$ or ln D_s vs. $\{1/T-\langle 1/T\rangle\}$, the brackets ($\langle\ \rangle$) indicating an average value. They are linear. The estimates of $\Delta H°$ and $\Delta G°_{Thm}$ for the retention equilibrium were calculated as $\Delta H° = -R$ (slope) and $\Delta G°_{Thm} = -RT_{hm}$ (intercept), respective-

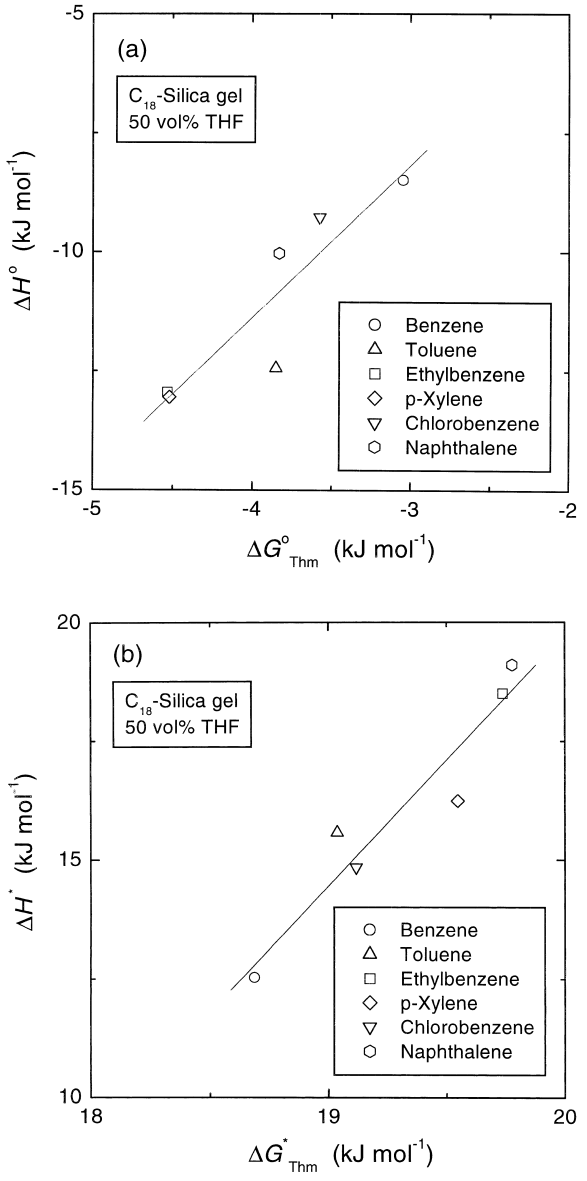

Fig. 10. Correlation between the free energy change at the harmonic mean of the experimental temperatures and the enthalpy change of (a) the retention equilibrium and (b) the surface diffusion.

ly. Similarly, ΔH^* and $\Delta G^*_{\mathrm{Thm}}$ for the surface diffusion were estimated as $\Delta H^* = -R$ (slope) $- RT_{\mathrm{hm}}$ and $\Delta G^*_{\mathrm{Thm}} = -RT_{\mathrm{hm}}$ (intercept) $+ (RT_{\mathrm{hm}} \ln [\lambda^2 e k_{\mathrm{B}} T_{\mathrm{hm}}/h] - RT_{\mathrm{hm}})$, respectively [46–48]. The value of λ was assumed to be $3 \cdot 10^{-8}$ cm from D_{s} data of the order of 10^{-6} cm^2 s^{-1} at 298 K.

(2) The second method consists in comparing T° and T_{hm} on the basis of the *t*-test (hypothesis test). The best estimate of T° should be sufficiently different from T_{hm}. The values of T° calculated were 430 K and 370 K for the retention equilibrium and surface diffusion, respectively. These values were derived from the slope of the linear correlation between ΔH° and $\Delta G^\circ_{\mathrm{Thm}}$ in Fig. 10a and that between ΔH^* and $\Delta G^*_{\mathrm{Thm}}$ in Fig. 10b, according to $T^\circ = T_{\mathrm{hm}}/[1 - 1/(\mathrm{slope})]$. These values of T° are rather close to the value of $T_{\mathrm{hm}} = 298$ K in this study. However, applying the *t*-test to these data shows that the hypothesis of a coincidence of the slope of the ΔH–ΔS plot (T°) with T_{hm} can be rejected at confidence levels of about 10% and 2% for the retention equilibrium and for surface diffusion, respectively. The relatively large value for the retention equilibrium is probably due to the discrepancy of a few plots from the linear correlation in Fig. 10a.

(3) The third method consists in checking that the Van't Hoff or Arrhenius plots do intersect at each corresponding T°.

Figs. 2 and 8 show the Van't Hoff plots of ln K vs. $1/T$ and the Arrhenius plots of ln D_{s} vs. $1/T$, respectively. The linear regression lines intersect approximately, although not in a single point but in a small region of the plane, due to the influence of experimental errors. In this study, the values of K and D_{s} were measured at three different temperatures, with a relatively narrow range compared with the difference between the intersection points and the experimental temperatures. This may explain the distribution of the intersection points. The compensation temperature estimated from the intersection points in Figs. 2 and 8 are fairly close to the values of T° obtained as described above (No. 2).

(4) Finally, according to the *F*-test, the probability that this intersection takes place should be compared with that for a nonintersection, on the basis of the statistical data derived by an analysis of variance (ANOVA) procedure [48]. The probability for nonintersection should also be compared to the precision of the experimental data in the same manner.

The values of the mean sum of squares were calculated according to the ANOVA procedure [48]. For both the retention equilibrium and surface diffusion, the mean sum of squares of the intersection

(MS_{con}) was one or two orders of magnitude larger than that of the nonintersection (MS_{noncon}). The ratio MS_{con}/MS_{noncon} is several times larger than the F-value, $F(1,4,1-\alpha=0.975)=12.2$, indicating that the probability of intersection is much higher than that of nonintersection. Similarly, the ratio of MS_{noncon} to the mean sum of squares of the residuals (MS_e) is much smaller than the corresponding F-value, $F(4,5,1-\alpha=0.975)=7.39$. The probability for nonconcurrence is smaller than the precision of the experimental data.

On the basis of the results described above, we conclude that the linear correlations in Figs. 3 and 9 between ln K_0 and Q_{st} and ln D_{s0} and E_s account for the real enthalpy–entropy compensation originating from physico–chemical effects taking place in the RPLC system.

As shown in Table 2, E_s is larger than $-Q_{st}$. Many similar experimental results were reported for surface diffusion in RPLC and in other liquid–solid adsorption systems [11,12,49–54]. The presence of surface diffusion is unexpected under such conditions because it is energetically more advantageous for the adsorbed molecules to be desorbed from the surface of C_{18}-silica gel particles into the bulk mobile phase than for them to migrate along the surface. In previous papers [10–12,22,52,55,56], we attempted quantitatively to interpret these unreasonable results from the following two points of view.

The first approach is through the influence of the mobile phase solvent on Q_{st} in RPLC. An analysis of the Q_{st} values based on the solvophobic theory showed that $|Q_{st}|$ measured in liquid–solid adsorption systems is smaller than that obtained in corresponding gaseous systems [11,22]. The second approach is through the thermodynamic properties of surface diffusion. By analyzing thermodynamic data concerning the retention behavior and surface diffusion in RPLC, we derived a surface-restricted molecular diffusion model as a second approximation of surface diffusion on the basis of the absolute rate theory [10–12,52,55,56]. This model is useful for interpreting some thermodynamic characteristics and the mass transfer mechanism of surface diffusion. A consistent interpretation was derived for the unreasonable correlation between E_s and Q_{st} described above.

In this model, E_s is assumed to consist of two contributions, originating from a hole-making and a bond-breaking step, respectively [11,55]. The activation energy of these steps may be correlated with the vaporization energy of the solvent (ΔE_v) and with the adsorption energy of the sample molecule, $-Q_{st}$, respectively. The proportionality constants were respectively estimated as ca. 0.47 and 0.4. The activation energy of the hole-making step is estimated at about 15 to 20 kJ mol^{-1}, because ΔE_v of various common solvents, e.g., water, alcohols, and aromatic hydrocarbons, is usually between ca. 30 and 40 kJ mol^{-1}. When Q_{st} is -20 kJ mol^{-1}, calculation gives $E_s=23$ to 28 kJ mol^{-1}. In this case, E_s would be larger than $-Q_{st}$. By contrast, if Q_{st} is -50 kJ mol^{-1}, E_s is approximately 35 to 40 kJ mol^{-1}, because the activation energy of the bond-breaking step is now estimated to be equal to about 20 kJ mol^{-1}, suggesting that the ratio $E_s/(-Q_{st})$ would be smaller than unity. It is likely that the unreasonable correlation between E_s and $-Q_{st}$ depends on the value of Q_{st}. When $-Q_{st}$ is larger than about 35 kJ mol^{-1}, E_s seems to be smaller than $-Q_{st}$. The result of this hypothetical calculation is supported by some previous experimental data, giving values of $-Q_{st}$ larger than about 40 kJ mol^{-1} and of $E_s/(-Q_{st})$ smaller than unity [53,54,57,58]. On the other hand, values of $E_s/(-Q_{st})$ larger than unity are frequently observed in RPLC because $-Q_{st}$ is usually smaller than the critical value of $-Q_{st}$, i.e., about 35 kJ mol^{-1} [11,12,52].

Fig. 11 indicates that ln D_s is linearly correlated with the boiling point of the sample compounds (T_b). The abscissa of the plot is the ratio of T_b to an experimental temperature (T). The solid line for 50% (v/v) THF at 298 K is represented by the following equation:

$$\ln D_s = -2.0\frac{T_b}{T} - 10.4 \quad (7)$$

Eq. (7) corresponds to the conventional Arrhenius equation. Comparison of Eqs. (6) and (7) suggests that E_s in Eq. (6) can be expressed as follows:

$$E_s = 2.0RT_b \quad (8)$$

On the other hand, the heat of vaporization (ΔH_v) is related to T_b according to the Trouton's rule:

$$\Delta H_v = 88T_b \quad (9)$$

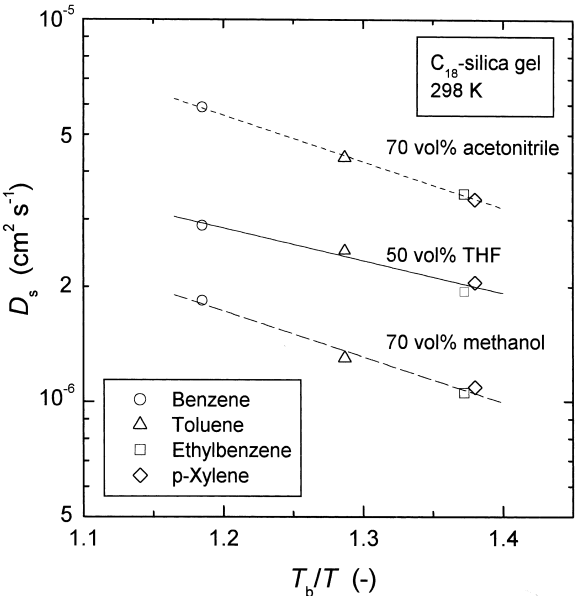

Fig. 11. Plot of surface diffusion coefficient against the ratio of boiling point to experimental temperature.

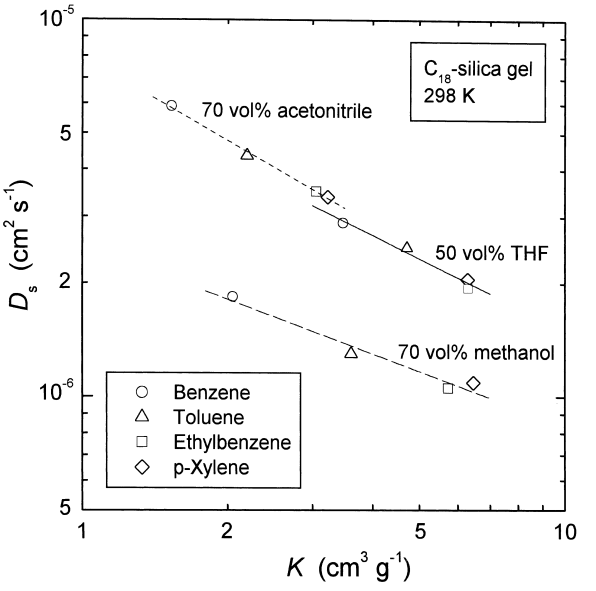

Fig. 12. Surface diffusion coefficient as a function of adsorption equilibrium constant.

As shown earlier in Eq. (2), the ratio $-Q_{st}/\Delta H_v$ was found to be ca. 0.35. As a consequence, Q_{st} is also related to T_b:

$$-Q_{st} = (0.35)\cdot(88)T_b \quad (10)$$

A comparison of Eqs. (8) and (10) suggests that E_s is approximately equal to 0.54 times $-Q_{st}$ in the RPLC system studied here. Fig. 11 also shows linear correlations for the other two systems, with 70% (v/v) methanol and 70% (v/v) acetonitrile. Although the values of D_s are different, the three straight lines are almost parallel to each other, suggesting that the ratio $E_s/(-Q_{st})$ is nearly the same in the three RPLC systems. These results suggest that E_s is smaller than $-Q_{st}$ in RPLC as in gas–solid adsorption systems [41].

Fig. 12 shows a linear correlation between ln D_s and ln K (a linear free-energy relationship) at 298 K in the three RPLC systems. The straight line for 50% (v/v) THF is almost the same as that for 70% (v/v) acetonitrile. Its equation is:

$$\ln D_s = -0.63(\ln K) - 12.0 \quad (11)$$

The absolute value of the slopes is close to 0.63, roughly equal to the ratio of $E_s/(-Q_{st})$ in RPLC [52]. This result is consistent with the value of $E_s/(-Q_{st})$ calculated above from the slope of the linear correlation between ln D_s and the ratio T_b/T in Fig. 11, i.e., 0.53, and with experimental observations made on gas–solid adsorption systems [41]. An almost parallel correlation is observed for 70% (v/v) methanol, although D_s in this case is smaller than for the other two solvents. We conclude from the analyses of the correlations between ln D_s and ln K and between ln D_s and T_b/T that E_s is smaller than $-Q_{st}$ in RPLC as well as in gas–solid adsorption systems.

4. Conclusion

Using THF, methanol, and acetonitrile, it was possible to prepare three similar RPLC systems for which the retention factors of a few aromatic hydrocarbons were close. The characteristics of the mass transfer kinetics of these compounds in the three systems showed that, in all cases, the three main mass transfer processes axial dispersion, fluid-to-particle mass transfer, and intraparticle diffusion, contribute nearly equally to band broadening for large particles. Surface diffusion plays the major role

in intraparticle diffusion. The values of D_s for the compounds studied increase in the order: methanol< THF<acetonitrile. However, the manner and degree of the influence of the nature of the organic modifier are different on D_s and on K, Q_{st}, $\Delta A/A_s$, and E_s.

The validity of several characteristic correlations was confirmed, independently of the type of the organic modifier used. These are an enthalpy–entropy compensation for both the retention behavior and surface diffusion, and a linear free-energy relationship. These linear correlations, however, do not always agree together. The linear correlations between ln D_s and ln K and between ln D_s and T_b/T suggest that E_s is smaller than $-Q_{st}$ in RPLC. In conclusion, the chromatographic retention mechanisms involved in these three RPLC systems seem to be similar, irrespective of the nature of the organic modifier. Obviously, the numerical values of the parameters characterizing retention and mass transfer are different and depend on the mobile phase composition.

5. Nomenclature

ΔA	Reduction of total hydrophobic surface area due to adsorption (cm^2)
A_s	Hydrophobic surface area of the sample molecule (cm^2)
d_p	Particle diameter (μm)
D	Diffusivity ($cm^2\ s^{-1}$)
D_e	Intraparticle diffusivity ($cm^2\ s^{-1}$)
D_L	Axial dispersion coefficient ($cm^2\ s^{-1}$)
D_m	Molecular diffusivity ($cm^2\ s^{-1}$)
D_p	Pore diffusivity ($cm^2\ s^{-1}$)
D_s	Surface diffusion coefficient ($cm^2\ s^{-1}$)
D_{s0}	Frequency factor of surface diffusion ($cm^2\ s^{-1}$)
e	Base of the natural logarithm
E_s	Activation energy of surface diffusion (kJ mol^{-1})
ΔE_v	Evaporation energy (J mol^{-1})
ΔG_{Thm}	Free energy change at T_{hm} (kJ mol^{-1})
h	Planck constant (J s)
ΔH	Enthalpy change (kJ mol^{-1})
ΔH_v	Heat of vaporization (kJ mol^{-1})
k	Tortuosity factor
k'	Retention factor
k_B	Boltzmann constant (J K^{-1})
k_f	Fluid-to-particle mass transfer coefficient (cm s^{-1})
K	Adsorption equilibrium constant ($cm^3\ g^{-1}$)
K_0	K at $1/T=0$ or $Q_{st}=0$ ($cm^3\ g^{-1}$)
MS_{con}	Mean sum of squares of the concurrence
MS_{noncon}	Mean sum of squares of the nonconcurrence
MS_e	Mean sum of squares of the residuals
Q_{st}	Isosteric heat of adsorption (J mol^{-1})
R	Gas constant (J $mol^{-1}\ K^{-1}$)
ΔS	Entropy change (J $mol^{-1}\ K^{-1}$)
T	Absolute temperature (K)
T_b	Boiling point (K)
T_{hm}	Harmonic mean of experimental temperatures (K)
T°	Compensation temperature (K)
u_0	Superficial velocity of the mobile phase (cm s^{-1})
V_b	Molar volume at normal boiling point ($cm^3\ mol^{-1}$)

Greek

δ	Contribution of mass transfer resistance to μ_2'
ϵ	Void fraction of the column
ϵ_p	Porosity of the stationary phase particle
η	Viscosity (Pa s)
λ	Distance between two equilibrium positions (cm)
μ_1	First moment (s)
μ_2'	Second central moment (s^2)
ρ_p	Particle density (g cm^{-3})

Subscripts

a	Solute
ads	Actual adsorption/desorption
ax	Axial dispersion
d	Intraparticle diffusion
f	Fluid-to-particle mass transfer
sv	Solvent

Acknowledgements

This work was supported in part by a Grant-in-

Aids for Scientific Research (No. 12640581) from the Japanese Ministry of Education, Science and Culture, by Grant CHE-00-70548 of the National Science Foundation, and by the cooperative agreement between the University of Tennessee and the Oak Ridge National Laboratory.

References

[1] G. Guiochon, S. Golshan-Shirazi, A.M. Katti, Fundamentals of Preparative and Nonlinear Chromatography, Academic Press, Boston, MA, 1994.
[2] A.M. Krstulovic, P.R. Brown, Reversed-Phase Liquid Chromatography, Wiley, New York, 1982.
[3] L.R. Snyder, J.L. Glajch, J.J. Kirkland, Practical HPLC Method Development, Wiley, New York, 1988.
[4] E. Kucera, J. Chromatogr. 19 (1965) 237.
[5] M. Kubin, Collect. Czech Chem. Commun. 30 (1965) 2900.
[6] E. Grushka, M.N. Myers, P.D. Schettler, J.C. Giddings, Anal. Chem. 41 (1969) 889.
[7] E. Grushka, J. Phys. Chem. 76 (1972) 2586.
[8] D.M. Ruthven, Principles of Adsorption and Adsorption Processes, Wiley, New York, 1984.
[9] M. Suzuki, Adsorption Engineering, Kodansha/Elsevier, Tokyo, 1990.
[10] K. Miyabe, G. Guiochon, Anal. Chem. 71 (1999) 889.
[11] K. Miyabe, G. Guiochon, Adv. Chromatogr. 40 (2000) 1.
[12] K. Miyabe, G. Guiochon, J. Phys. Chem. B 103 (1999) 11086.
[13] E.J. Wilson, C.J. Geankoplis, Ind. Eng. Chem. Fundam. 5 (1966) 9.
[14] R.C. Reid, J.M. Prausnitz, T.K. Sherwood, The Properties of Gases and Liquids, McGraw-Hill, New York, 1977.
[15] K. Miyabe, G. Guiochon, Anal. Chem. 72 (2000) 5162.
[16] T. Kataoka, H. Yoshida, K. Ueyama, J. Chem. Eng. Jpn. 5 (1972) 132.
[17] A. Bondi, J. Phys. Chem. 68 (1964) 441.
[18] O. Sinanoglu, in: B. Pullman (Ed.), Molecular Associations in Biology, Academic Press, New York, 1968, p. 427.
[19] T. Halicioglu, O. Sinanoglu, Ann. N.Y. Acad. Sci. 158 (1969) 308.
[20] C. Horváth, W. Melander, I. Molnar, J. Chromatogr. 125 (1976) 129.
[21] G. Belfort, G.L. Altshuler, K.K. Thallam, C.P. Feerick Jr., K.L. Woodfield, AIChE J. 30 (1984) 197.
[22] K. Miyabe, M. Suzuki, AIChE J. 41 (1995) 536.
[23] K. Miyabe, S. Takeuchi, Anal. Chem. 69 (1997) 2567.
[24] J.H. Knox, G. Vasvari, J. Chromatogr. 83 (1973) 181.
[25] H. Colin, G. Guiochon, J. Chromatogr. 141 (1977) 289.
[26] C. Horváth, W. Melander, J. Chromatogr. Sci. 15 (1977) 393.
[27] H. Colin, G. Guiochon, J. Chromatogr. 158 (1978) 183.
[28] H. Colin, J.C. Diez-Masa, G. Guiochon, T. Czajkowska, I. Miedziak, J. Chromatogr. 167 (1978) 41.
[29] K.K. Unger, in: Porous Silica, Elsevier, Amsterdam, 1979, p. 122.
[30] H.J. Issaq, M. Jaroniec, J. Liq. Chromatogr. 12 (1989) 2067.
[31] K. Miyabe, M. Suzuki, AIChE J. 41 (1995) 548.
[32] W.R. Melander, D.E. Campbell, C. Horváth, J. Chromatogr. 158 (1978) 215.
[33] W.R. Melander, B.K. Chen, C. Horváth, J. Chromatogr. 185 (1979) 99.
[34] K.B. Woodburn, L.S. Lee, P.S.C. Rao, J.J. Delfino, Environ. Sci. Technol. 23 (1989) 407.
[35] C.M. Riley, E. Tomlinson, T.M. Jefferies, J. Chromatogr. 185 (1979) 197.
[36] C.M. Riley, E. Tomlinson, T.L. Hafkenscheid, J. Chromatogr. 218 (1981) 427.
[37] P.K. de Bokx, H.M.J. Boots, J. Phys. Chem. 93 (1989) 8243.
[38] J. Li, P.W. Carr, J. Chromatogr. A 670 (1994) 105.
[39] H.M.J. Boots, P.K. de Bokx, J. Phys. Chem. 93 (1989) 8240.
[40] A. Vailaya, C. Horváth, J. Phys. Chem. 100 (1996) 2447.
[41] K. Miyabe, M. Suzuki, AIChE J. 39 (1993) 1791.
[42] J.C. Giddings, Dynamics of Chromatography, Part I, Principles and Theory, Marcel Dekker, 1965.
[43] H.C. Chen, S.H. Chen, Ind. Eng. Chem. Fundam. 24 (1985) 183.
[44] N. Tanaka, K. Kimata, K. Hosoya, H. Miyanishi, T. Araki, J. Chromatogr. A 656 (1993) 265.
[45] K. Miyabe, M. Suzuki, Ind. Eng. Chem. Res. 33 (1994) 1972.
[46] R.R. Krug, W.G. Hunter, R.A. Grieger, J. Phys. Chem. 80 (1976) 2335.
[47] R.R. Krug, W.G. Hunter, R.A. Grieger, J. Phys. Chem. 80 (1976) 2341.
[48] R.R. Krug, Ind. Eng. Chem. Fundam. 19 (1980) 50.
[49] F. Awum, S. Narayan, D. Ruthven, Ind. Eng. Chem. Res. 27 (1988) 1510.
[50] Y.H. Ma, Y.S. Lin, H.L. Fleming, AIChE Symp. Ser. 84 (1988) 1.
[51] C.B. Chiang, K. Hidajat, M.S. Uddin, Sep. Sci. Technol. 24 (1989) 581.
[52] K. Miyabe, G. Guiochon, Anal. Chem. 72 (2000) 1475.
[53] H. Komiyama, J.M. Smith, AIChE J. 20 (1974) 728.
[54] A. Itaya, Y. Fujita, N. Kato, K. Okamoto, J. Chem. Eng. Jpn. 20 (1987) 638.
[55] K. Miyabe, S. Takeuchi, J. Phys. Chem. B 101 (1997) 7773.
[56] K. Miyabe, S. Takeuchi, AIChE J. 43 (1997) 2997.
[57] M. Suzuki, T. Fujii, AIChE J. 28 (1982) 380.
[58] M. Muraki, Y. Iwashita, T. Hayakawa, J. Chem. Eng. Jpn. 15 (1982) 34.